Productivity and evapotranspiration of two contrasting semiarid ecosystems following the 2011 global carbon land sink anomaly

James CLEVERLY*[a,b], Derek EAMUS[a,b], Eva VAN GORSEL[c], Chao CHEN[a,1], Rizwana RUMMAN[a], Qunying LUO[d], Natalia RESTREPO COUPE[d], Longhui LI[a], Natascha KLJUN[e], Ralph FAUX[a], Qiang YU[a] and Alfredo HUETE[d]

[a] School of Life Sciences, University of Technology Sydney, PO Box 123, Broadway, NSW, 2007, Australia

[b] Australian Supersite Network, Terrestrial Ecosystem Research Network, University of Technology Sydney, PO Box 123, Broadway, NSW, 2007, Australia

[c] CSIRO Oceans and Atmosphere, Forestry House, Building 002, Wilf Crane Crescent, Yarralumla, ACT 2601, Australia

[d] Climate Change Cluster, University of Technology Sydney, PO Box 123, Broadway, NSW, 2007, Australia

[e] Department of Geography, Swansea University, Singleton Park, Swansea SA2 8PP, UK

*Correspondence: James.Cleverly@UTS.edu.au, +61 (02) 9514 8405, +61 (02) 9514 4079 (FAX)

Keywords: ***Corymbia*** **savanna;** ***Acacia*** **woodland; evapotranspiration; net ecosystem productivity; water-use efficiency; global 2011 land sink anomaly**

[1] Present address: CSIRO Agriculture Flagship, PMB 5, PO Wembley, WA, 6913, Australia

ABSTRACT

Global carbon balances are increasingly affected by large fluctuations in productivity occurring throughout semiarid regions. Recent analyses found a large C uptake anomaly in 2011 in arid and semiarid regions of the southern hemisphere. Consequently, we compared C and water fluxes of two distinct woody ecosystems (a Mulga (*Acacia*) woodland and a *Corymbia* savanna) between August 2012 and August 2014 in semiarid central Australia, demonstrating that the 2011 anomaly was short-lived in both ecosystems. The Mulga woodland was approximately C neutral but with periods of significant uptake within both years. The extreme drought tolerance of *Acacia* is presumed to have contributed to this. By contrast, the *Corymbia* savanna was a very large net C source (130 and 200 g C m^{-2} yr^{-1} in average and below average rainfall years, respectively), which is likely to have been a consequence of the degradation of standing, senescent biomass that was a legacy of high productivity during the 2011 anomaly. The magnitude and temporal patterns in ecosystem water-use efficiencies (WUE), derived from eddy covariance data, differed across the two sites, which may reflect differences in the relative contributions of respiration to net C fluxes across the two ecosystems. In contrast, differences in leaf-scale measures of WUE, derived from ^{13}C stable isotope analyses, were apparent at small spatial scales and may reflect the different rooting strategies of *Corymbia* and *Acacia* trees within the *Corymbia* savanna. Restrictions on root growth and infiltration by a siliceous hardpan located below *Acacia*, whether in the Mulga woodland or in small Mulga patches of the *Corymbia* savanna, impedes drainage of water to depth, thereby producing a reservoir for soil moisture storage under *Acacia* while acting as a barrier to access of groundwater by *Corymbia* trees in Mulga patches, but not in the open *Corymbia* savanna.

1. Introduction

Inter-annual variability in atmospheric concentrations of CO_2 is large (Le Quéré et al., 2014), and much of this variability is driven by fluctuations in the source/sink strength of terrestrial ecosystems (Cox et al., 2013). During the latter half of the twentieth century, global net primary productivity (NPP) may have increased (Nemani et al., 2003), resulting in a potential increase in uptake of 0.05 Pg C per year (Ballantyne et al., 2012). Then, global NPP was reduced by 0.55 Pg C during the period 2000–2009, a result ascribed to large-scale drought in the southern hemisphere (Zhao and Running, 2010). Thereafter, Le Quéré et al. (2014) identified the 2011 land sink anomaly, which was a year of exceptional productivity, and Poulter et al. (2014) confirmed this anomaly by using a combination of modelling and remote sensing approaches. This land sink anomaly was driven by growth in semiarid vegetation of the southern hemisphere, with almost 60% occurring in Australia (Poulter et al., 2014). Importantly, Fasullo et al. (2013) showed that Australia, unlike continental South and North America, maintained a positive water mass anomaly (i.e., the extra water received in 2011 remained detectable throughout 2012), suggesting that increased C uptake may have persisted beyond 2011 in arid Australia. Carry-over of water from one hydrologic year to the next has been shown to have strong positive effects on productivity in many arid ecosystems (Flanagan and Adkinson, 2011). We have previously shown, using field observations of landscape fluxes of CO_2, that one of the dominant ecosystems of semiarid central Australia was indeed a large sink for C over almost all of the 12 months between October 2010 and October 2011 (Cleverly et al., 2013a; Eamus et al., 2013). Large fluctuations in productivity, evapotranspiration (ET) and ecosystem water-use efficiency (eWUE) across these semiarid regions reflect the very high ecosystem resilience of vegetation (Ponce Campos et al., 2013), which can have large

70 effects on global C relations and consequently drive events such as the land sink anomaly
71 of 2011.
72 Globally, dryland regions (arid, semiarid, and subhumid) cover 41% of the land
73 area (Reynolds et al., 2007). Within these regions, arid and semiarid environments are
74 characterised by chronic water shortages. Thus, productivity and ET are closely
75 dependent upon the timing, frequency and amount of precipitation (Huxman et al., 2004),
76 through which plant water availability is mediated by local hydrology (Breshears et al.,
77 2009; Loik et al., 2004; Reynolds et al., 2004).
78 The semiarid regions of Australia cover 70% of the continent (Eamus et al., 2006;
79 Warner, 2004) and are dominated by three major biomes along a woodland-savanna-
80 grassland continuum: (1) Mulga woodlands (*Acacia* spp.), which cover approximately
81 20–25% of the continental land area (Bowman et al., 2008), and (2) *Corymbia* savanna
82 over a hummock grass (*Triodia* spp.) understorey that grades into (3) treeless hummock
83 grasslands. Hummock grasslands and savannas occupy another 20–25% of the Australian
84 land surface (Bowman et al., 2008). The co-occurrence of two widely distributed and
85 highly distinctive vegetation types (i.e., Mulga and hummock) within a single climate
86 zone in central Australia (O'Grady et al., 2009) provides an opportunity to compare and
87 contrast their behaviour and to establish their respective contributions to regional C, water
88 and energy budgets.
89 Mulga trees range in height (2–10 m) and ground cover (10–70%) (Nix and
90 Austin, 1973), and they are preferentially located where storage of soil moisture occurs
91 near the surface in sand dunes, clay-rich soil or over the siliceous hardpans that are
92 common across semiarid Australia (Bowman et al., 2007; Ludwig et al., 2005; Maslin and
93 Reid, 2012; Nano and Clarke, 2010; Nix and Austin, 1973; Thiry et al., 2006; Tongway
94 and Ludwig, 1990). In contrast, tree density (stems per hectare) and cover in *Corymbia*

savannas are very low, and tree height ranges from 5–15 m. *Corymbia opaca* is deep-rooted (8–20 m), and tends to be groundwater dependent in semiarid areas (Cook and O'Grady, 2006; O'Grady et al., 2006a; O'Grady et al., 2006b). The understory in the *Corymbia* savanna is characterised by a continuous cover of perennial hummock grasses (*Triodia* spp.), which are widespread throughout Australia and cover an additional 20–25% of the continental land area (Bowman et al., 2008; Nano and Clarke, 2010; Reid et al., 2008).

Water-use-efficiency (WUE) has traditionally been measured at leaf-scales (as the ratio of net assimilation to transpiration), but eddy covariance measurements also allow determination of ecosystem-scale WUE as the ratio of net ecosystem productivity (NEP) to ET (eWUE; Eamus et al., 2013). Given the very large difference in LAI of the C_4 grass understory between Mulga and *Corymbia* savannas, we hypothesised that ecosystem-scale WUE of the two biomes would differ. Furthermore, given the large differences in phyllode structure of the C_3 trees, comparisons of leaf-scale measures of WUE across two co-occurring species within a *single* biome (i) provide information about C and water economies and (ii) contribute to our understanding of hydraulic niche separation of co-occurring species (Peñuelas et al., 2011) that cannot be addressed through eWUE.

The aim of this study was to investigate fluctuations in the fluxes of C and water from iconic Australian semiarid vegetation in response to reductions in precipitation subsequent to the 2011 land sink anomaly. In this manuscript we compare and contrast the behaviour of two disparate arid-zone tropical ecosystems (Mulga woodland and *Corymbia* savanna) in central Australia to address four over-arching questions: (a) did the 2011 anomaly persist into 2012/2013/2014 in either biome; (b) do these two contrasting ecosystems respond similarly to almost identical weather patterns; (c) how do ecosystem water-use efficiencies compare across ecosystems; and (d) at small spatial scales within

120 the *Corymbia* savanna, how do leaf-scale water-use efficiencies across the two tree species
121 (*Acacia* and *Corymbia*) differ?
122
123 **2. Materials and Methods**
124 **2.1. Site descriptions**
125 This study was located on Pine Hill cattle station in the Ti Tree catchment of
126 central Australia and was co-located with several previous hydrological, ecological and
127 ecophysiological studies (Calf et al., 1991; Cleverly et al., 2013a; Eamus et al., 2013;
128 Harrington et al., 2002; Ma et al., 2013; O'Grady et al., 2009; Scanlon et al., 2006). The
129 Ti Tree catchment is an enclosed basin that covers 5,500 km^2 and contains two main
130 ecosystems: Mulga woodlands and *Corymbia* savanna (Harrington et al., 2002).
131 Measurements were collected from two locations: one in the Mulga woodland and one in
132 the *Corymbia* savanna. An eddy covariance tower was located in each ecosystem,
133 separated by 40 km at the same latitude ([22.3 °S 133.25 °E] and [22.3 °S 133.65 °E]).
134 A full description of the soil, floristics, leaf area index (LAI), energy balance and
135 C relations of the Mulga woodland can be found in Cleverly et al. (2013a) and Eamus et
136 al. (2013). Briefly, the Mulga woodland is characterised by a discontinuous canopy of
137 short (3–7 m), evergreen *Acacia* trees (*A. aptaneura* and *A. aneura*) with an understorey
138 of shrubs, herbs and grasses (C_3 and C_4) that are conditionally active depending upon
139 moisture availability and season (Cleverly et al., 2013a). The cover of *Acacia* is 74.5 % of
140 the land area in the Mulga woodland; *C. opaca* is essentially absent from the Mulga
141 woodland (one tree within the EC footprint, cf. Section 2.2). The basal area of *Acacia*
142 within the woodland is 8 m^2 ha^{-1} (Eamus et al., 2013).
143 The second eddy covariance site contains two species of trees: widely spaced and
144 tall *Corymbia opaca* trees above a matrix of hummock grass (Spinifex, *Triodia schinzii*)

and small patches of Mulga (*A. sericophylla*, *A. melleodora* and *A. aptaneura*) that contain an understorey of herbs and tussock grasses (*Aristida* spp., *Eremophila latrobei* subsp. *glabra*, *Eragrostis eriopoda* subsp. *red earth*, *Paraneurachne muelleri* and *Psydrax latifolia*). Although the distribution of *T. schinzii* does not substantially overlap with Mulga, *C. opaca* trees were present in both habitats. Representing only 0.4 % cover (basal area of 0.21 m^2 ha^{-1}), *C. opaca* are found predominantly in the open savanna, although they are found occasionally in the isolated small Mulga patch close to the EC tower within in the *Corymbia* savanna. Soil texture is sandier in the *Corymbia* savanna (loamy sand) than in the Mulga woodland (sandy loam). Soil organic matter is less than 1% at both sites. In the *Corymbia* savanna, the energy balance ratio $(H + LE)/(R_n - G)$ was 0.97 ± 0.005 (January 2013–July 2014), wherein H is sensible heat flux, LE is latent heat flux, R_n is net radiation and G is ground heat flux. Over the same period in the Mulga woodland, the energy balance ratio was 0.89 ± 0.005. The Bowen ratio (H/LE) was large at both sites: 37.5 (range 0.78–408) in the Mulga woodland and 37.9 (0.23–511) in the *Corymbia* savanna.

Long-term annual average precipitation (1987–2014) at the nearest meteorological station (Territory Grape Farm, 18 km due south of the *Corymbia* savanna site) is 320.7 mm (http://www.bom.gov.au). The monsoon tropics of Australia are defined by the receipt of 85% of annual precipitation during the November–April monsoon season (Bowman et al., 2010), which places these sites within the monsoon zone on average (Cleverly et al., 2013a). However, during the first 16 months of this study (August 2012–November 2013), very little rain was received and there was consequently negligible grassy understorey, in contrast to the extensive understorey that was present during the land sink anomaly of 2011 (Eamus et al., 2013).

2.2. Eddy covariance data

Eddy covariance analyses of NEP and ET were used as measures of net C uptake and ecosystem water use. In the eddy covariance method, ET is determined from the covariance between vertical wind speed (w) and specific humidity (q): $ET = \langle w'q' \rangle / \rho_w$, where $\langle\ \rangle$ represents an average in time and the prime operator represents the deviation from a mean: $q' = \langle q \rangle - q_i$. Similarly, NEP was taken to be the negative covariance between w and $[CO_2]$ (c): $NEP = -\langle w'c' \rangle$. By this definition, NEP is positive during C uptake (i.e., photosynthesis, C sink) and negative for net C emissions (C source). The trade-off between C uptake and ET was represented by eWUE, which was calculated as the ratio of NEP and ET. Because of non-linearity at very small values of ET, eWUE was determined only when ET was larger than 0.2 mm d^{-1}.

Both tower sites are part of the OzFlux Network (Cleverly, 2011; Cleverly, 2013). The 90% flux footprint (Kljun et al., 2004) under turbulent conditions extended 200–300 m to the southeast of either tower, although variability in roughness length across the *Corymbia* savanna interferes with the reliability of footprint estimates at that site. In the *Corymbia* savanna, approximately 25% of the flux footprint covered the *Corymbia* savanna, while the remaining 75% of the footprint was located over the small Mulga patch that included *Acacia*, *Corymbia* and tussock grasses. The trees nearest the tower in the open *Corymbia* savanna are *Acacia* with a canopy height of 4.85 m, in contrast to the 6.5 m tall *Acacia* in the Mulga woodland. Thus, measurements were made over the *Corymbia* savanna at a slightly lower height (9.85 m) than above the Mulga woodland (11.6 m, Cleverly et al., 2013a). Where possible, the instruments on each tower were the same (e.g., Campbell Scientific CSAT3) or only different in the model of sensor (e.g., Kipp & Zonen CNR1 *v*. CNR4, Li-Cor 7500 *v.* 7500A), in which the newer models were used in the *Corymbia* savanna.

All estimates of error were determined as the standard error (s.e. = $\sigma / n^{0.5}$, where σ is the standard deviation and n is sample size).

2.2.1. Quality control, corrections and gap-filling

Quality control of meteorological and flux measurements (QA/QC) was performed on both towers as described in Eamus et al. (2013). Briefly, QA/QC procedures included spike detection and removal, range checks that include rejection of measurements when the wind was from a 90° arc behind the sonic anemometer (CSAT3) and tower (10% of observations, only during the passage of frontal systems that generate advection and negative fluxes of LE; Beringer and Tapper, 2000), and filtering for bad measurements of humidity from the IRGA in comparison to a slow-response sensor. Corrections included 2-dimensional coordinate rotation (Wesely, 1970), frequency attenuation correction for time averaging and sensor displacement (Massman and Clement, 2004), conversion of virtual to actual sensible heat flux (Campbell Scientific Inc., 2004; Schotanus et al., 1983), correction for flux-density effects (the Webb, Pearman and Leuning correction, which accounts for density effects arising from heat and water vapour fluxes; Webb et al., 1980) and storage of heat in the soil above the ground heat flux plates. Corrections and QA/QC steps were performed using OzFluxQC and the OzFluxQC Simulator, both in version 2.8.5 and available online (e.g., Cleverly and Isaac, 2015). Gaps in fluxes were filled using a self-organising linear output (SOLO) that was trained on a self-organising feature map (SOFM) of meteorological (net radiation, air temperature, vapour pressure deficit, specific humidity) and soil measurements (G, soil temperature, soil moisture content at the surface) (Eamus et al., 2013). SOLO is a statistical artificial neural network (ANN) and was chosen for its resistance to overtraining (Hsu et al., 2002), ability to simulate fluxes

219 (Abramowitz et al., 2006), and small RMSE relative to feed forward ANNs (Eamus et al.,
220 2013).

221 In contrast to gaps in the flux measurements, two types of gaps were identified in
222 the meteorological data: those that were due to measurement over-ranging on the
223 datalogger and those that occurred during system maintenance. Over-ranging was
224 identified in the measurement of solar radiation during periods when reflection from a
225 cloud face generated large (> 1200 W m^{-2}) radiant fluxes. To avoid underestimation bias
226 in these cases, gaps in 30-minute solar (R_s) and net (R_n) radiation were filled from the
227 measured value in each minute that did not report an over-ranging error (26–29 one-
228 minute values). These gaps first occurred during the summer 2012–2013 at the *Corymbia*
229 savanna site, after which modifications to the datalogger prevented re-occurrence of solar
230 spike gaps.

231 System maintenance gaps were typically 30–300 minutes and did not coincide
232 among sites. Filling of gaps in the meteorological variables that were used as predictors
233 for gap filling of fluxes was performed using several methods: 1) linear interpolation, 2)
234 replacement of measurements from the companion tower, and 3) SOLO-SOFM trained on
235 measurements from the paired tower. Gaps in meteorological measurements were filled
236 using the method that produced the smallest disjunction at gap boundaries.

237

238 **2.3. Trends in satellite derived enhanced vegetation index (EVI) for the two sites**

239 The moderate resolution imaging spectroradiometer (MODIS) enhanced vegetation
240 index (EVI) is sensitive to vegetation "greenness" (i.e., chlorophyll content) and structural
241 properties (e.g., LAI, canopy type, plant physiognomy, canopy architecture) (Huete et al.,
242 2002). Thus, the satellite product MODIS EVI was used in this study to assess structural
243 and functional responses of the vegetation. The MOD13Q1 product was retrieved from

244 the ORNL DAAC depository at a temporal resolution of 16 days and a spatial resolution
245 of 250 m. Values were composited into a single 9 × 9 pixel centred on each tower (2.25
246 km resolution, only pixels that passed QA at 100% were used). The MODIS satellite was
247 launched in 2000, and we present the entire record to provide context for the ecosystem
248 dynamics observed over this two-year study.
249
250 **2.4. ^{13}C foliar stable isotopes**
251 To compare leaf-scale intrinsic WUE (WUE_i) at small spatial scales within the
252 *Corymbia* savanna, leaf samples were collected in September 2013 for analysis of the
253 stable isotope ratio of C ($\delta^{13}C$). Mature leaves of *Corymbia opaca* and *Acacia* trees were
254 collected from three habitats within the *Corymbia* savanna. The first habitat was from the
255 *Corymbia* savanna *per se*; the second habitat was the small Mulga patch close to the EC
256 tower within the *Corymbia* savanna; the third habitat was the transition between the small
257 Mulga patch and the *Corymbia* savanna. For comparison with *Acacia* sampled within the
258 *Corymbia* savanna, $\delta^{13}C$ of bulk leaf tissue was also measured in the Mulga woodland
259 from two replicate branches of three replicate trees of *Acacia*.
260 In *Corymbia*, three leaves from different branches were collected. Each leaf was
261 ground and subsampled to obtain three representative independent values per tree.
262 Likewise, *Acacia* phyllodes were sampled from three different branches, although several
263 phyllodes were combined from each branch due to their small size. The C isotopic
264 composition was measured using a Picarro G2121-i Analyser for Isotopic CO_2 (Picarro
265 Inc., Santa Clara CA USA). Atropine and acetanilide were used as internal reference
266 standards and calibrated against international measurement standards sucrose (IAEA-CH-
267 6, $\delta^{13}C_{VPDB} = -10.45$ ‰), cellulose (IAEA-CH-3, $\delta^{13}C_{VPDB} = -24.72$ ‰) and graphite
268 (USGS24, $\delta^{13}C_{VPDB} = -16.05$ ‰). Values of $\delta^{13}C$ in bulk leaf samples represent an

integrated value of C_i / C_a (i.e., the ratio of internal leaf and atmospheric CO_2 density) during the entire age of the leaf.

3. Results

3.1. Water fluxes: daily, seasonal and annual precipitation

Daily rainfall across the two-year period showed minimal differences between the Mulga woodland and *Corymbia* savanna sites (Fig. 1a, b). Rainfall in both years was concentrated between November and early May, although both sites received about 12 mm of rain in July 2014. During the first year of this study (2013–2014), rainfall during the monsoon season (November–April) was 71 and 74% of total annual rainfall for that year in the Mulga woodland and *Corymbia* savanna, respectively. In the following year, rainfall during the monsoon season was 92% of total annual rainfall at both sites. Although these sites are within the monsoon zone on average (Cleverly et al., 2013a), the monsoon did not penetrate inland to the location of these sites in the first year of the present study (August 2012–July 2013). Due to the proximity between sites, annual rainfall did not differ in either of the two years of the present study. Likewise, due to cross-correlation between precipitation *versus* temperature (maximum, mean, minimum), solar radiation and vapour pressure deficit (Cleverly et al., 2013a), meteorological conditions were equivalent across sites (data not shown).

In the 2010–2011 hydrological year (August–July), annual rainfall (565 mm) was significantly larger than the long-term average of 320.7 mm (Table 1). In contrast, annual rainfall was smaller than average in hydrological years 2011–2013 (Table 1). During the first year of this study (August 2012–July 2013), annual rainfall was approximately 40% less than the long-term average (192.8 and 190.6 mm in the Mulga woodland and *Corymbia* savanna, respectively). In the second year of this study (2013–2014), rainfall

294 was 294.6 and 289.8 mm in the Mulga woodland and *Corymbia* savanna, respectively
295 (approximately 8% below the long-term average). Monthly patterns and cumulative
296 annual (August–July) rainfall in the first year of study were almost identical at the two
297 sites (Fig. 1c). In contrast there was more rain earlier in the second hydrologic year
298 (November 2013–February 2014) at the *Corymbia* savanna than the Mulga woodland,
299 although annual totals for the two sites did not differ.
300
301 **3.2. Water fluxes: evapotranspiration**
302 Patterns in daily ET were similar across the two-year study at both sites (Fig. 2a)
303 and closely followed those observed for rainfall. Daily ET at both sites was negligible
304 during those periods when daily rainfall was zero for more than two weeks (e.g., August
305 2012 and 2013, June 2014). Maximum rates of daily ET from the *Corymbia* savanna were
306 either equal to or frequently larger (by up to approximately 80%) than those from the
307 Mulga woodland (Fig. 2a). Summer total and maximum daily rates of ET were larger in
308 the second summer than in the first at both sites. As with rainfall, 73 and 88% of ET was
309 lost from the Mulga woodland during the first and second monsoon seasons, respectively.
310 Likewise in the *Corymbia* savanna, 71 and 91% of ET was lost during the respective
311 monsoon seasons.
312 In both hydrologic years (August 2012–July 2014), patterns of cumulative ET
313 were broadly similar at the two sites, but with a consistent difference in the total amount
314 of ET (Fig. 2b). Moreover, the annual sum of ET was smaller for the Mulga woodland
315 than the *Corymbia* savanna in both years. The annual total ET for the *Corymbia* savanna
316 was 96 and 110% of annual rainfall in each year (2012–2013 and 2013–2014,
317 respectively), but in the Mulga woodland the annual sum of ET was approximately 80%
318 of total rainfall in both years (cf. Figs. 1c and 2b). Immediately following precipitation,

there were larger pulses of ET from the *Corymbia* savanna than from the Mulga woodland (cf. Figs. 1c and 2a). These short imbalances were more prominent in the second year, when ET was 110% of precipitation in the *Corymbia* savanna.

3.3. Carbon fluxes: net productivity and water-use efficiency

In contrast to the very similar patterns in daily ET at both sites, patterns in daily NEP differed substantially between the two sites (Fig. 3a). During the winter and early spring (August–October) of 2012, the Mulga woodland was a small sink (NEP = 0.1 to 0.3 g C m^{-2} d^{-1}), but the *Corymbia* savanna was a moderate source for C (NEP = −0.6 to −0.3 g C m^{-2} d^{-1}). This pattern was repeated in the second winter/early spring (June–August 2013). The *Corymbia* savanna remained a moderate-to-strong source (NEP = −1.75 to −0.5 g C m^{-2} d^{-1}) between November 2012 and January 2014, with the exception of a short period during June 2013 when the *Corymbia* savanna became C neutral (uptake equalled release) (Fig. 3a). The *Corymbia* savanna was a sink for C (maximum daily NEP = 1.5 g C m^{-2} d^{-1}) for approximately six weeks in the summer of 2014 (late January to early March). The Mulga was a moderate-to-large C source for the spring and early summer of 2014 and became a moderate sink (maximum NEP = 0.75 g C m^{-2} d^{-1}) in late summer and autumn of 2014 (Fig. 3a).

During summer in the *Corymbia* savanna, the pulse of productivity was rapid and large following the largest storm in the two years of study (> 100 mm in January 2014; cf. Figs. 1 and 3a), and this was due to the dominant cover of C_4 grasses (90%). By contrast in the Mulga woodland, productivity was limited during the summer, acting as a source for several weeks until late summer and early autumn of 2014 (Fig. 3a). In contrast, both sites were a C source in January 2013 (Fig. 3a). During this time, ecosystem respiration at night was similarly small in the Mulga woodland and *Corymbia* savanna (Fig. 4).

However, during the sunlit hours, NEP diverged between the two sites. By example in January 2013 the Mulga woodland was a net C source. However, in the mornings of January, a positive NEP (C sink, reflecting a stimulation of photosynthetic C uptake through increased solar radiation input) was recorded, followed by a rapid decline from mid-morning through to early evening (Fig. 4). NEP was negative (C source) prior to sundown. By contrast, NEP was consistently negative in the *Corymbia* savanna, which was a stronger C source during daylight hours than at night, reflecting the enhanced rates of C emissions that occurred during sunlit hours in the savanna.

Cumulative annual NEP in both hydrologic years showed the *Corymbia* savanna to be a strong source (cumulative NEP = −197 and −131 g C m^{-2} y^{-1} for the first and second years, respectively; Fig. 3b). In contrast, the Mulga woodland was a small source (−26 g C m^{-2} y^{-1}) in the first hydrologic year but a small sink (12 g C m^{-2} y^{-1}) in the second year. It wasn't until the occurrence of a wet summer that the Mulga woodland again became a moderate-to-strong sink (0.9 g C m^{-2} d^{-1}), although annual C uptake was considerably less than that observed in the 2010–2011 anomaly (12 *versus* 259 g C m^{-2} y^{-1}), reflecting the non-linear response of NEP to total annual rainfall in this system. The trend in cumulative NEP at the two sites diverged in early March 2014, with the *Corymbia* savanna reverting to a source for the remaining five months of the study and the Mulga continuing as a net sink (Fig. 3b).

In the *Corymbia* savanna, eWUE was negative (negative because respiratory loss exceeded photosynthetic C gain) for most of the two years of study (Fig. 5) and was more negative in the first hydrologic year than the second. Periods of very small positive or slightly negative eWUE for the *Corymbia* coincided with the rainfall of November 2012–February 2013, May 2013 and January–March 2014. In contrast, the Mulga woodland maintained near-zero values of eWUE in both years, although eWUE increased gradually

in autumn (March – May) as soil water stores that were recharged during the wet season declined following the cessation of summer rainfall (Fig. 5).

3.4. Trends in enhanced vegetation index and foliar ^{13}C stable isotope contents

MODIS EVI exhibited strong peaks at the study sites in five of 13 years since the launch of the satellite: March 2000, April 2001, April 2007, March 2010 and March 2011 (Fig. 6). In a given year, neither ecosystem consistently responded to precipitation with more production of green tissue than the other (Fig. 6). While MODIS EVI was generally larger in the Mulga woodland than in the *Corymbia* savanna, two periods (2004 and 2010) when this pattern was reversed are apparent (Fig. 6). Note that during the first year of this study (2012–2013), MODIS EVI values were the smallest on record for the Mulga woodland and as small as previous minima in the *Corymbia* savanna (2008, 2009).

In *Acacia* phyllodes, $\delta^{13}C$ values averaged −27.9‰ and did not differ substantially across the two sites and in the three habitats sampled within the *Corymbia* savanna. By contrast, $\delta^{13}C$ in *Corymbia opaca* leaves declined substantially across habitats (Fig. 7). Leaf $\delta^{13}C$ of the *Corymbia* trees declined in the sequence: *Corymbia* trees in the Mulga patch within the *Corymbia* savanna > *Corymbia* trees in the transition between the *Acacia* patch and open *Corymbia* savanna > *Corymbia* trees in the extensive open savanna (Fig. 7). Leaf $\delta^{13}C$ in *Corymbia* was less negative than in *Acacia* phyllode in the Mulga patch (Fig. 7).

4. Discussion

4.1. The 2011 anomaly and beyond

Although measurements were not initiated in the *Corymbia* savanna until after the conclusion of the land sink anomaly, C fluxes in subsequent years can only be explained

394 within the context of the land sink anomaly. Several lines of field-based evidence support
395 the conclusion (Le Quéré et al., 2014; Poulter et al., 2014) that Australian semi-arid
396 vegetation had a major role in the large global land sink anomaly of 2011. First, our field-
397 based studies of CO_2 fluxes in central Australia (Table 1; Eamus et al., 2013)
398 demonstrated that the Mulga woodland was indeed a large sink for C (259 g C m^{-2} y^{-1},
399 Table 1) during that year (September 2010–August 2011; Eamus et al., 2013). This sink
400 formed in response to a disproportionate increase in gross primary production (GPP, 793 g
401 C m^{-2} y^{-1}) relative to the moderate increase in ecosystem respiration (Cleverly et al.,
402 2013a). Second, the largest value of EVI since 2000 was observed in hydrologic year
403 2010–2011 (Ma et al., 2013), which suggests as large a C sink in the *Corymbia* savanna as
404 in the Mulga woodland due to the close correlation between EVI and GPP across tropical
405 and semi-arid Australia (Donohue et al., 2014; Ma et al., 2013; Ma et al., 2014). Third,
406 2010–2011 was identified as having the largest rates of ET in the Ti Tree basin since 1981
407 (Chen et al., 2014). Finally, the Gravity Recovery and Climate Experiment (GRACE)
408 satellite data recorded significant increases in the amount of water stored across the
409 Australian landmass in 2011 (Boening et al., 2012), coincident with the extremely large
410 La Niña conditions that dominated weather across Australia in that year.
411 During the global land sink anomaly of 2011, rainfall at our sites was almost
412 double the long-term average (565 mm *versus* 320.7 mm, 1987–2014), resulting in very
413 large rates of ecosystem productivity in the Mulga woodland (Eamus et al., 2013) and the
414 *Corymbia* savanna (Fig. 6). Across a range of biomes, different combinations of rainfall,
415 temperature, solar radiation and vapour pressure deficit are the principle determinants of
416 NEP and GPP (Baldocchi, 2008; Baldocchi and Ryu, 2011; Kanniah et al., 2010; van Dijk
417 et al., 2005; Zha et al., 2013). It is apparent that inter-annual differences in precipitation
418 are the principle causes of interannual differences in sink strength for the Mulga woodland

(Table 1), in strong agreement with multiple other arid and semiarid biomes (Barron-Gafford et al., 2012; Chen et al., 2014; Flanagan and Adkinson, 2011; Huxman et al., 2004; Ma et al., 2012) but in marked contrast to boreal forests, tropical montane forests, temperate mesic deciduous forests and tropical mesic savannas, where temperature, solar radiation and the length of the growing season are the principal factors limiting NEP (Baldocchi, 2008; Dunn et al., 2007; Keenan et al., 2014; Luyssaert et al., 2007; Ma et al., 2013; Whitley et al., 2011; Zha et al., 2013). We now discuss the question: did this anomaly persist into 2012–2014 for our two study sites?

Despite the persistence of anomalously large moisture reserves in Australia through 2012 (Fasullo et al., 2013), the productivity pulse of 2011 (Eamus et al., 2013) did not persist in either ecosystem following the conclusion of the 2011 global land C sink anomaly. Productivity declined in the Mulga woodland by July 2011, which was four months following the end of the summer rains (Cleverly et al., 2013a; Eamus et al., 2013), and the Mulga woodland was effectively C neutral (i.e., near zero within the limits of measurement uncertainty) in the three following years (2012–2014). The ratio of GPP to ecosystem respiration fell between 2011 and 2012, reflecting a two-fold decline in annual GPP (Cleverly et al., 2013a) and a four-fold decline in the seasonal peak of daily GPP (Ma et al., 2013). Similarly, there was little evidence of productivity in the *Corymbia* savanna during the first nine months of the current study (August 2012–May 2013). In pyrophytic landscapes such as the *Corymbia* savanna, large amounts of fuel can accumulate following very wet periods (King et al., 2013; Schlesinger et al., 2013). However, large rates of C loss from this biome during subsequent dry years imply a rapid loss of fuel load via photodegradation. Thus, *Corymbia* savannas that do not burn in the first few years following very wet conditions are less likely to burn thereafter.

444 **4.2. *Corymbia* savanna *versus* Mulga woodland**

445 In this section, we address the question: how do current behaviours of the Mulga
446 woodland (in terms of CO_2 and water fluxes) compare to those of an adjacent, floristically
447 different, *Corymbia* savanna?

448 Some of the ET excess in the *Corymbia* savanna in the second year of study (ET =
449 110% of precipitation) arose from precipitation that fell during the first year but
450 contributed to second-year ET, while the remainder may illustrate the opportunistic use of
451 groundwater by *Corymbia* trees in the open savanna during short periods of cloud cover,
452 cool temperatures, and low VPD that accompany rainfall. What was perhaps surprising
453 was the continued ET deficit in the Mulga woodland (about 80% of annual rainfall) in the
454 very wet (2011) year (Eamus et al., 2013) and the subsequent dry years, with little
455 apparent use of water that was carried-over in soil storage, in marked contrast to the
456 generally positive effect of carry-over of water from one year to the next in arid zones
457 (Flanagan and Adkinson, 2011). However, the abundant sunshine and soil moisture
458 availability during the summer of 2013–2014 may suggest that ET was limited by
459 stomatal responses to high temperature and large VPD (Cleverly et al., 2013b) rather than
460 energy or water availability. Thus, recharge and discharge of soil moisture storage (and
461 the ratio of ET to precipitation) vary on longer timescales than the scope of our
462 measurements, in contrast to the intra-annual carry-over of water from the wet season into
463 the cool season observed in North American drylands (Hastings et al., 2005). In both
464 ecosystems, the increase in evaporative fraction (defined as the ratio of ET to net
465 radiation) from the first to the second summer was the result of higher ET and lower net
466 radiation during the second summer. This difference between summer seasons was the
467 consequence of disparities in the amount and temporal distribution of rainfall. In the

second summer, larger storms and fewer sunny days caused VPD to be much smaller, with a consequential reduction in leaf stress.

The resilience of both ecosystems (*sensu* Ponce Campos et al., 2013, where resilience is defined as ecophysiological drought tolerance that does not diminsh photosynthetic responses to subsequent periods of favourable moisture availability) resulted in large fluctuations of eWUE and a near-neutral annual C balance in the Mulga woodland (Fig. 3 and Cleverly et al., 2013a), whereas the C cycle in the *Corymbia* savanna was dominated by large C losses (Fig. 3). Two reasons may be postulated to explain the difference in C balance of the two sites. First, *Acacia* has a suite of traits that are indicative of a high degree of drought tolerance compared to *Corymbia*: larger wood density, smaller specific leaf area (SLA, ratio of leaf area to leaf dry mass) and larger Huber value (ratio of sapwood cross-sectional area to leaf area) (O'Grady et al., 2009). Large wood densities are strongly correlated with enhanced resistance to xylem embolism, reduced soil-to-leaf hydraulic conductance and small transpiration rates (Wright et al., 2006; Zhang et al., 2009), while a small SLA correlates with an ability to tolerate lower (more negative) canopy water potentials. As a result, small rates of productivity in the Mulga woodland were sufficient for maintaining C neutrality. Second, woody plants dominate the Mulga woodland, whereas the contribution of *Acacia* and *Corymbia* to the cover, basal area and LAI of the *Corymbia* savanna is small relative to the extensive C_4 grasses. We propose that the large amount of standing dead biomass in the *Corymbia* savanna (accumulated during the 2011 anomaly) was subject to physical fragmentation by photodegradation (i.e., in the presence of light, e.g. Fig. 4, and absence of soil moisture; Rutledge et al., 2010; Vanderbilt et al., 2008).

492 **4.3. Ecosystem-scale water use efficiency (eWUE) and small-scale differences in**
493 **foliar WUE (WUE_i)**

494 By delaying production until the autumn of 2014, eWUE in the Mulga woodland
495 was larger than in the *Corymbia* savanna. In addition to the traits of drought tolerance,
496 which are correlated to large WUE, the large foliar N content of the nitrogen fixing *Acacia*
497 allows for significant resource substitution, whereby larger-than-expected rates of
498 photosynthesis can be sustained in arid environments through preferential allocations of
499 nitrogen to Rubisco (Taylor and Eamus, 2008). When stomatal conductance and
500 transpiration rates decline in response to large VPD, resource substitution results in large
501 eWUE. Further, spatial variability in soil properties (especially the distribution of the
502 hardpan) restricts soil moisture availability (Chen et al., 2014) and contributes to large
503 values of eWUE in the Mulga woodland.

504 It is important to note that the eWUE of the Mulga woodland consistently showed
505 that photosynthetic C uptake exceeded respiratory loss per unit ET during the early or late
506 summer and autumn of both years, as previously observed by Eamus et al. (2013). The
507 very low values of eWUE in the *Corymbia* savanna imply that C source strength was
508 maintained regardless of moisture status, thus eWUE became much more negative during
509 dry periods than eWUE in the Mulga woodland (Fig. 5). These predominantly large,
510 negative values of eWUE (respiration exceeds C gain per unit ET) in the *Corymbia*
511 savanna are further symptomatic of photodegradation. Despite the differences in eWUE
512 between ecosystems and the plants that co-exist in them, eWUE in the Mulga woodland
513 and the *Corymbia* savanna showed large fluctuations between wet and dry periods that
514 reflected differences in the moisture requirements of photosynthesis, autotrophic and
515 microbial respiration, and photodegradation.

In leaves of *Corymbia* across all three habitats, declining leaf $\delta^{13}C$ represents increased access to water and declining WUE_i (Leffler and Evans, 1999; Zolfaghar et al., 2014) and has been previously used to infer access to groundwater (Zolfaghar et al., 2014). We interpret this as reflecting an increasing rooting depth of *Corymbia* trees within the *Corymbia* savanna when moving into the extensive open savanna from the Mulga patch. The potential for groundwater access by deeply rooted *Corymbia* in the extensive savanna, where groundwater depth is approximately 8 m, is presumably large and may explain the lower WUE_i of *Corymbia*, while the presence of an inferred hardpan within the Mulga patch prevents access to the water table and hence an increased WUE_i for *Corymbia* within the Mulga patch. The absence of any significant change in phyllode $\delta^{13}C$ for the *Acacia* at any of the three locations within the *Corymbia* savanna reflects the shallow rooting habit of *Acacia* (Pressland, 1975). More importantly, there was no difference in foliar ^{13}C content of *Acacia* sampled from the Mulga woodland where groundwater depth is known to exceed 50 m, further supporting the conclusion that access to groundwater by Mulga within the *Corymbia* savanna is not occurring. The low values of $\delta^{13}C$ in *Acacia* phyllodes are consistent with their anisohydric stomatal responses to soil drying; that is, their stomata remain open even at very low water potentials (O'Grady et al., 2009; Winkworth, 1973).

5. Conclusions

We have demonstrated that the large 2011 anomaly in terrestrial C uptake was short-lived in the arid zone of central Australia. In the Mulga woodland, storage of soil moisture within the root zone contributed to C neutrality (i.e., C sources were equivalent to sinks) in the subsequent drier-than-average years by facilitating the delayed response of productivity to precipitation. We also demonstrated that productivity in the Mulga

541 woodland was larger than that of the *Corymbia* savanna in the drier-than-average years of
542 the study and attributed this to the multiple drought tolerant attributes and the larger
543 potential for resource substitution of *Acacia* compared to *Corymbia*. Drought tolerance in
544 the Mulga woodland further restricted ET to 80% of precipitation in each year since 2010,
545 indicating that variations in soil moisture storage occur over very long timescales. In
546 contrast, ET from the *Corymbia* savanna was larger than precipitation in the near-average
547 rainfall year, illustrating that groundwater use by *Corymbia* occurred opportunistically
548 during wet periods. However, the *Corymbia* savanna was a strong source of CO_2 in drier-
549 than-average and near-average years due to photodegradation of the extensive grassy
550 understorey. Finally, we demonstrated that ecosystem water-use efficiency was larger in
551 the Mulga woodland than in the *Corymbia* savanna, while differences in leaf/phyllode
552 $\delta^{13}C$ between *Acacia* and *Corymbia* reflected differential access to groundwater and the
553 different rooting characteristics of these two tree species.
554
555

6. Acknowledgements

This work was supported by grants from the Australian Government's Terrestrial Ecosystems Research Network (TERN, www.tern.gov), the National Centre for Groundwater Research and Training (NCGRT), and the Australian Research Council. We would like to thank Emrys Leitch for providing taxonomic identifications.

7. References

Abramowitz, G., Gupta, H., Pitman, A., Wang, Y., Leuning, R., Cleugh, H. and Hsu, K.L., 2006. Neural Error Regression Diagnosis (NERD): A tool for model bias identification and prognostic data assimilation. J. Hydrometeor. 7: 160–177.

Baldocchi, D., 2008. Breathing of the terrestrial biosphere: lessons learned from a global network of carbon dioxide flux measurement systems. Aust. J. Bot. 56: 1–26, DOI: 10.1071/BT07151.

Baldocchi, D.D. and Ryu, Y., 2011. A synthesis of forest evaporation fluxes – from days to years – as measured with eddy covariance. In: D.F. Levia, D. Carlyle-Moses and T. Tanaka (Editors), Forest Hydrology and Biogeochemistry: Synthesis of Past Research and Future Directions. Ecological Studies. Springer, Dordrecht, Netherlands, pp. 101–116, DOI: 10.1007/978-94-007-1363-5_5.

Ballantyne, A.P., Alden, C.B., Miller, J.B., Tans, P.P. and White, J.W.C., 2012. Increase in observed net carbon dioxide uptake by land and oceans during the past 50 years. Nature. 488: 70–73, DOI: 10.1038/nature11299.

Barron-Gafford, G.A., Scott, R.L., Jenerette, G.D., Hamerlynck, E.P. and Huxman, T.E., 2012. Temperature and precipitation controls over leaf- and ecosystem-level CO_2 flux along a woody plant encroachment gradient. Glob. Change Biol. 18: 1389–1400, DOI: 10.1111/j.1365-2486.2011.02599.x.

Beringer, J. and Tapper, N.J., 2000. The influence of subtropical cold fronts on the surface energy balance of a semi-arid site. J. Arid. Environ. 44: 437-450.

Boening, C., Willis, J.K., Landerer, F.W., Nerem, R.S. and Fasullo, J., 2012. The 2011 La Niña: So strong, the oceans fell. Geophys. Res. Lett. 39, DOI: 10.1029/2012gl053055.

Bowman, D., Boggs, G.S. and Prior, L.D., 2008. Fire maintains an *Acacia aneura* shrubland—*Triodia* grassland mosaic in central Australia. J. Arid. Environ. 72: 34–47, DOI: 10.1016/j.jaridenv.2007.04.001.

Bowman, D., Boggs, G.S., Prior, L.D. and Krull, E.S., 2007. Dynamics of *Acacia aneura-Triodia* boundaries using carbon (^{14}C and $\delta^{13}C$) and nitrogen ($\delta^{15}N$) signatures in soil organic matter in central Australia. Holocene. 17: 311–318, DOI: 10.1177/0959683607076442.

Bowman, D., Brown, G.K., Braby, M.F., Brown, J.R., Cook, L.G., Crisp, M.D., Ford, F., Haberle, S., Hughes, J., Isagi, Y., Joseph, L., McBride, J., Nelson, G. and Ladiges, P.Y., 2010. Biogeography of the Australian monsoon tropics. J. Biogeogr. 37: 201–216, DOI: 10.1111/j.1365-2699.2009.02210.x.

Breshears, D.D., Myers, O.B. and Barnes, F.J., 2009. Horizontal heterogeneity in the frequency of plant-available water with woodland intercanopy-canopy vegetation patch type rivals that occuring vertically by soil depth. Ecohydrology. 2: 503–519.

Calf, G.E., McDonald, P.S. and Jacobson, G., 1991. Recharge mechanism and groundwater age in the Ti-Tree basin, Northern Territory. Aust. J. Earth Sci. 38: 299–306, DOI: 10.1080/08120099108727974.

Campbell Scientific Inc., 2004. Open path eddy covariance system operator's manual, Logan, UT, USA, pp. 60.

Chen, C., Eamus, D., Cleverly, J., Boulain, N., Cook, P., Zhang, L., Cheng, L. and Yu, Q., 2014. Modelling vegetation water-use and groundwater recharge as affected by climate variability in an arid-zone *Acacia* savanna woodland. J. Hydrol. 519: 1084–1096, DOI: 10.1016/j.jhydrol.2014.08.032.

Cleverly, J., 2011. Alice Springs Mulga OzFlux site. OzFlux: Australian and New Zealand Flux Research and Monitoring Network, hdl: 102.100.100/8697.

Cleverly, J., 2013. Ti Tree East OzFlux Site. OzFlux: Australian and New Zealand Flux Research and Monitoring Network, hdl: 102.100.100/11135.

Cleverly, J., Boulain, N., Villalobos-Vega, R., Grant, N., Faux, R., Wood, C., Cook, P.G., Yu, Q., Leigh, A. and Eamus, D., 2013a. Dynamics of component carbon fluxes in a semi-arid *Acacia* woodland, central Australia. J. Geophys. Res.-Biogeosci. 118: 1168–1185, DOI: 10.1002/jgrg.20101.

Cleverly, J., Chen, C., Boulain, N., Villalobos-Vega, R., Faux, R., Grant, N., Yu, Q. and Eamus, D., 2013b. Aerodynamic resistance and Penman-Monteith evapotranspiration over a seasonally two-layered canopy in semiarid central Australia. J. Hydrometeor. 14: 1562–1570, DOI: 10.1175/jhm-d-13-080.1.

Cleverly, J. and Isaac, P., 2015. OzFluxQC Simulator version 2.8.6. GitHub respository, github.com/james-cleverly/OzFluxQC_Simulator, DOI: 10.5281/zenodo.13730.

Cook, P.G. and O'Grady, A.P., 2006. Determining soil and ground water use of vegetation from heat pulse, water potential and stable isotope data. Oecologia. 148: 97–107, DOI: 10.1007/s00442-005-0353-4.

Cox, P.M., Pearson, D., Booth, B.B., Friedlingstein, P., Huntingford, C., Jones, C.D. and Luke, C.M., 2013. Sensitivity of tropical carbon to climate change constrained by carbon dioxide variability. Nature. 494: 341–344, DOI: 10.1038/nature11882.

Donohue, R.J., Hume, I.H., Roderick, M.L., McVicar, T.R., Beringer, J., Hutley, L.B., Gallant, J.C., Austin, J.M., van Gorsel, E., Cleverly, J.R., Meyer, W.S. and Arndt, S.K., 2014. Evaluation of the remote-sensing-based DIFFUSE model for estimating photosynthesis of vegetation. Remote Sens. Environ. 155: 349–365, DOI: 10.1016/j.rse.2014.09.007.

Dunn, A.L., Barford, C.C., Wofsy, S.C., Goulden, M.L. and Daube, B.C., 2007. A long-term record of carbon exchange in a boreal black spruce forest: means, responses to interannual variability, and decadal trends. Glob. Change Biol. 13: 577–590, DOI: 10.1111/j.1365-2486.2006.01221.x.

Eamus, D., Cleverly, J., Boulain, N., Grant, N., Faux, R. and Villalobos-Vega, R., 2013. Carbon and water fluxes in an arid-zone *Acacia* savanna woodland: An analyses of seasonal patterns and responses to rainfall events. Agric. For. Meteor. 182–183: 225–238, DOI: 10.1016/j.agrformet.2013.04.020.

Eamus, D., Hatton, T., Cook, P. and Colvin, C., 2006. Ecohydrology. Vegetation function, water and resource management. CSIRO Publishing, Collingwood, VIC, 348 pp.

Fasullo, J.T., Boening, C., Landerer, F.W. and Nerem, R.S., 2013. Australia's unique influence on global sea level in 2010-2011. Geophys. Res. Lett. 40: 4368-4373, DOI: 10.1002/grl.50834.

Flanagan, L.B. and Adkinson, A.C., 2011. Interacting controls on productivity in a northern Great Plains grassland and implications for response to ENSO events. Glob. Change Biol. 17: 3293–3311, DOI: 10.1111/j.1365-2486.2011.02461.x.

Harrington, G.A., Cook, P.G. and Herczeg, A.L., 2002. Spatial and temporal variability of ground water recharge in central Australia: A tracer approach. Ground Water. 40: 518–527, DOI: 10.1111/j.1745-6584.2002.tb02536.x.

Hastings, S.J., Oechel, W.C. and Muhlia-Melo, A., 2005. Diurnal, seasonal and annual variation in the net ecosystem CO_2 exchange of a desert shrub community (Sarcocaulescent) in Baja California, Mexico. Glob. Change Biol. 11: 927–939, DOI: 10.1111/j.1365-2486.2005.00951.x.

Hsu, K.-l., Gupta, H.V., Gao, X., Sorooshian, S. and Imam, B., 2002. Self-organizing linear output map (SOLO): An artificial neural network suitable for hydrologic modeling and analysis. Water Resour. Res. 38: 1302, DOI: 10.1029/2001wr000795.

Huete, A., Didan, K., Miura, T., Rodriguez, E.P., Gao, X. and Ferreira, L.G., 2002. Overview of the radiometric and biophysical performance of the MODIS vegetation indices. Remote Sens. Environ. 83: 195–213, DOI: 10.1016/s0034-4257(02)00096-2.

Huxman, T.E., Snyder, K.A., Tissue, D., Leffler, A.J., Ogle, K., Pockman, W.T., Sandquist, D.R., Potts, D.L. and Schwinning, S., 2004. Precipitation pulses and carbon fluxes in semiarid and arid ecosystems. Oecologia. 141: 254–268, DOI: 10.1007/s00442-004-1682-4.

Kanniah, K.D., Beringer, J. and Hutley, L.B., 2010. The comparative role of key environmental factors in determining savanna productivity and carbon fluxes: A review, with special reference to Northern Australia. Progress in Physical Geography. 34: 459–490.

Keenan, T.F., Gray, J., Friedl, M.A., Toomey, M., Bohrer, G., Hollinger, D.Y., Munger, J.W., O'Keefe, J., Schmid, H.P., Wing, I.S., Yang, B. and Richardson, A.D., 2014. Net carbon uptake has increased through warming-induced changes in temperate forest phenology. Nature Clim. Change. 4: 598–604, DOI: 10.1038/nclimate2253.

King, K.J., Cary, G.J., Bradstock, R.A. and Marsden-Smedley, J.B., 2013. Contrasting fire responses to climate and management: insights from two Australian ecosystems. Glob. Change Biol. 19: 1223–1235, DOI: 10.1111/gcb.12115.

Kljun, N., Calanca, P., Rotach, M.W. and Schmid, H.P., 2004. A simple parameterisation for flux footprint predictions. Bound.-Lay. Meteor. 112: 503-523, DOI: 10.1023/b:boun.0000030653.71031.96.

Le Quéré, C., Peters, G.P., Andres, R.J., Andrew, R.M., Boden, T.A., Ciais, P., Friedlingstein, P., Houghton, R.A., Marland, G., Moriarty, R., Sitch, S., Tans, P., Arneth, A., Arvanitis, A., Bakker, D.C.E., Bopp, L., Canadell, J.G., Chini, L.P., Doney, S.C., Harper, A., Harris, I., House, J.I., Jain, A.K., Jones, S.D., Kato, E., Keeling, R.F., Klein Goldewijk, K., Körtzinger, A., Koven, C., Lefèvre, N., Maignan, F., Omar, A., Ono, T., Park, G.H., Pfeil, B., Poulter, B., Raupach, M.R., Regnier, P., Rödenbeck, C., Saito, S., Schwinger, J., Segschneider, J., Stocker, B.D., Takahashi, T., Tilbrook, B., van Heuven, S., Viovy, N., Wanninkhof, R., Wiltshire, A. and Zaehle, S., 2014. Global carbon budget 2013. Earth Syst. Sci. Data. 6: 235–263, DOI: 10.5194/essd-6-235-2014.

Leffler, A.J. and Evans, A.S., 1999. Variation in carbon isotope composition among years in the riparian tree *Populus fremontii*. Oecologia. 119: 311–319.

Loik, M.E., Breshears, D.D., Lauenroth, W.K. and Belnap, J., 2004. A multi-scale perspective of water pulses in dryland ecosystems: climatology and ecohydrology of the western USA. Oecologia. 141: 269–281.

Ludwig, J.A., Wilcox, B.P., Breshears, D.D., Tongway, D.J. and Imeson, A.C., 2005. Vegetation patches and runoff-erosion as interacting ecohydrological processes in semiarid landscapes. Ecology. 86: 288–297.

Luyssaert, S., Inglima, I., Jung, M., Richardson, A.D., Reichstein, M., Papale, D., Piao, S.L., Schulzes, E.D., Wingate, L., Matteucci, G., Aragao, L., Aubinet, M., Beers, C., Bernhofer, C., Black, K.G., Bonal, D., Bonnefond, J.M., Chambers, J., Ciais, P., Cook, B., Davis, K.J., Dolman, A.J., Gielen, B., Goulden, M., Grace, J., Granier, A., Grelle, A., Griffis, T., Grunwald, T., Guidolotti, G., Hanson, P.J., Harding, R., Hollinger, D.Y., Hutyra, L.R., Kolar, P., Kruijt, B., Kutsch, W., Lagergren, F., Laurila, T., Law, B.E., Le Maire, G., Lindroth, A., Loustau, D., Malhi, Y., Mateus, J., Migliavacca, M., Misson, L., Montagnani, L., Moncrieff, J., Moors, E., Munger, J.W., Nikinmaa, E., Ollinger, S.V., Pita, G., Rebmann, C., Roupsard, O., Saigusa, N., Sanz, M.J., Seufert, G., Sierra, C., Smith, M.L., Tang, J., Valentini, R., Vesala, T. and Janssens, I.A., 2007. CO_2 balance of boreal, temperate, and tropical forests derived from a global database. Glob. Change Biol. 13: 2509–2537, DOI: 10.1111/j.1365-2486.2007.01439.x.

Ma, J., Zheng, X.J. and Li, Y., 2012. The response of CO_2 flux to rain pulses at a saline desert. Hydrol. Process. 26: 4029–4037, DOI: 10.1002/hyp.9204.

Ma, X., Huete, A., Yu, Q., Coupe, N.R., Davies, K., Broich, M., Ratana, P., Beringer, J., Hutley, L.B., Cleverly, J., Boulain, N. and Eamus, D., 2013. Spatial patterns and temporal dynamics in savanna vegetation phenology across the North Australian Tropical Transect. Remote Sens. Environ. 139: 97–115, DOI: 10.1016/j.rse.2013.07.030.

Ma, X., Huete, A., Yu, Q., Restrepo-Coupe, N., Beringer, J., Hutley, L.B., Kanniah, K.D., Cleverly, J. and Eamus, D., 2014. Parameterization of an ecosystem light-use-efficiency model for predicting savanna GPP using MODIS EVI. Remote Sens. Environ. 154: 253–271, DOI: 10.1016/j.rse.2014.08.025.

Maslin, B.R. and Reid, J.E., 2012. A taxonomic revision of Mulga (*Acacia aneura* and its close relatives: Fabaceae) in Western Australia. Nuytsia. 22: 129–167.

Massman, W. and Clement, R., 2004. Uncertainty in eddy covariance flux estimates resulting from spectral attenuation. In: X. Lee, W. Massman and B. Law (Editors), Handbook of Micrometeorology: A guide for Surface Flux Measurement and Analysis. Atmospheres and Oceanographic Sciences Library. Kluwer Academic Publishers, Dordrecht/Boston/London, pp. 67–100.

Nano, C.E.M. and Clarke, P.J., 2010. Woody-grass ratios in a grassy arid system are limited by multi-causal interactions of abiotic constraint, competition and fire. Oecologia. 162: 719–732, DOI: 10.1007/s00442-009-1477-8.

Nemani, R.R., Keeling, C.D., Hashimoto, H., Jolly, W.M., Piper, S.C., Tucker, C.J., Myneni, R.B. and Running, S.W., 2003. Climate-driven increases in global terrestrial net primary production from 1982 to 1999. Science. 300: 1560–1563, DOI: 10.1126/science.1082750.

Nix, H.A. and Austin, M.P., 1973. Mulga: a bioclimatic analysis. Tropical Grasslands. 7: 9–20.

O'Grady, A.P., Cook, P.G., Eamus, D., Duguid, A., Wischusen, J.D.H., Fass, T. and Worldege, D., 2009. Convergence of tree water use within an arid-zone woodland. Oecologia. 160: 643–655, DOI: 10.1007/s00442-009-1332-y.

O'Grady, A.P., Cook, P.G., Howe, P. and Werren, G., 2006a. Groundwater use by dominant tree species in tropical remnant vegetation communities. Aust. J. Bot. 54: 155–171, DOI: 10.1071/bt04179.

O'Grady, A.P., Eamus, D., Cook, P.G. and Lamontagne, S., 2006b. Comparative water use by the riparian trees *Melaleuca argentea* and *Corymbia bella* in the wet-dry tropics of northern Australia. Tree Physiol. 26: 219–228.

Peñuelas, J., Terradas, J. and Lloret, F., 2011. Solving the conundrum of plant species coexistence: water in space and time matters most. New Phytol. 189: 5-8, DOI: 10.1111/j.1469-8137.2010.03570.x.

Ponce Campos, G.E., Moran, M.S., Huete, A., Zhang, Y., Bresloff, C., Huxman, T.E., Eamus, D., Bosch, D.D., Buda, A.R., Gunter, S.A., Scalley, T.H., Kitchen, S.G., McClaran, M.P., McNab, W.H., Montoya, D.S., Morgan, J.A., Peters, D.P.C., Sadler, E.J., Seyfried, M.S. and Starks, P.J., 2013. Ecosystem resilience despite large–scale altered hydroclimate conditions. Nature. 494: 349–352, DOI: 10.1038/nature11836.

Poulter, B., Frank, D., Ciais, P., Myneni, R.B., Andela, N., Bi, J., Broquet, G., Canadell, J.G., Chevallier, F., Liu, Y.Y., Running, S.W., Sitch, S. and van der Werf, G.R., 2014. Contribution of semi-arid ecosystems to interannual variability of the global carbon cycle. Nature. 509: 600–603, DOI: 10.1038/nature13376.

Pressland, A.J., 1975. Productivity and management of Mulga in south-western Queensland in relation to tree structure and density. Aust. J. Bot. 23: 965–976, DOI: 10.1071/bt9750965.

763 Reid, N., Hill, S.M. and Lewis, D.M., 2008. Spinifex biogeochemical expressions
764 of buried gold mineralisation: The great mineral exploration penetrator of transported
765 regolith. Appl. Geochem. 23: 76–84, DOI: 10.1016/j.apgeochem.2007.09.007.

766 Reynolds, J.F., Kemp, P.R., Ogle, K. and Fernandez, R.J., 2004. Modifying the
767 'pulse-reserve' paradigm for deserts of North America: precipitation pulses, soil water, and
768 plant responses. Oecologia. 141: 194–210.

769 Reynolds, J.F., Stafford Smith, D.M., Lambin, E.F., Turner, B.L., Mortimore, M.,
770 Batterbury, S.P.J., Downing, T.E., Dowlatabadi, H., Fernandez, R.J., Herrick, J.E., Huber-
771 Sannwald, E., Jiang, H., Leemans, R., Lynam, T., Maestre, F.T., Ayarza, M. and Walker,
772 B., 2007. Global desertification: Building a science for dryland development. Science.
773 316: 847–851, DOI: 10.1126/science.1131634.

774 Rutledge, S., Campbell, D.I., Baldocchi, D. and Schipper, L.A., 2010.
775 Photodegradation leads to increased carbon dioxide losses from terrestrial organic matter.
776 Glob. Change Biol. 16: 3065–3074, DOI: 10.1111/j.1365-2486.2009.02149.x.

777 Scanlon, B.R., Keese, K.E., Flint, A.L., Flint, L.E., Gaye, C.B., Edmunds, W.M.
778 and Simmers, I., 2006. Global synthesis of groundwater recharge in semiarid and arid
779 regions. Hydrol. Process. 20: 3335–3370, DOI: 10.1002/hyp.6335.

780 Schlesinger, C., White, S. and Muldoon, S., 2013. Spatial pattern and severity of
781 fire in areas with and without buffel grass (*Cenchrus ciliaris*) and effects on native
782 vegetation in central Australia. Austral Ecol. 38: 831–840, DOI: 10.1111/aec.12039.

783 Schotanus, P., Nieuwstadt, F.T.M. and Debruin, H.A.R., 1983. Temperature-
784 measurement with a sonic anemometer and its application to heat and moisture fluxes.
785 Bound.-Lay. Meteor. 26: 81–93.

786 Taylor, D. and Eamus, D., 2008. Coordinating leaf functional traits with branch
787 hydraulic conductivity: resource substitution and implications for carbon gain. Tree
788 Physiol. 28: 1169–1177.

789 Thiry, M., Milnes, A.R., Rayot, V. and Simon-Coincon, R., 2006. Interpretation of
790 palaeoweathering features and successive silicifications in the Tertiary regolith of inland
791 Australia. J. Geol. Soc. 163: 723–736, DOI: 10.1144/0014-764905-020.

792 Tongway, D.J. and Ludwig, J.A., 1990. Vegetation and soil patterning in semiarid
793 mulga lands of Eastern Australia. Aust. J. Ecol. 15: 23–34, DOI: 10.1111/j.1442-
794 9993.1990.tb01017.x.

795 van Dijk, A., Dolman, A.J. and Schulze, E.D., 2005. Radiation, temperature, and
796 leaf area explain ecosystem carbon fluxes in boreal and temperate European forests. Glob.
797 Biogeochem. Cycle. 19: GB2029, DOI: 10.1029/2004gb002417.

798 Vanderbilt, K.L., White, C.S., Hopkins, O. and Craig, J.A., 2008. Aboveground
799 decomposition in arid environments: Results of a long-term study in central New Mexico.
800 J. Arid. Environ. 72: 696–709.

Warner, T.T., 2004. Desert Meteorology. Cambridge University Press, Cambridge UK, 595 pp.

Webb, E., Pearman, G. and Leuning, R., 1980. Correction of flux measurements for density effects due to heat and water-vapor transfer. Q. J. Roy. Meteor. Soc. 106: 85–100.

Wesely, M.L., 1970. Eddy correlation measurements in the atmospheric surface layer over agricultural crops. Ph.D. Dissertation Thesis, University of Wisconsin, Madison, 102 pp.

Whitley, R.J., Macinnis-Ng, C.M.O., Hutley, L.B., Beringer, J., Zeppel, M., Williams, M., Taylor, D. and Eamus, D., 2011. Is productivity of mesic savannas light limited or water limited? Results of a simulation study. Glob. Change Biol. 17: 3130–3149, DOI: 10.1111/j.1365-2486.2011.02425.x.

Winkworth, R.E., 1973. Eco-physiology of Mulga (*Acacia aneura*). Tropical Grasslands. 7: 43–48.

Wright, I.J., Falster, D.S., Pickup, M. and Westoby, M., 2006. Cross-species patterns in the coordination between leaf and stem traits, and their implications for plant hydraulics. Physiologia Plantarum. 127: 445–456, DOI: 10.1111/j.1399-3054.2006.00699.x.

Zha, T.S., Li, C.Y., Kellomaki, S., Peltola, H., Wang, K.Y. and Zhang, Y.Q., 2013. Controls of evapotranspiration and CO_2 fluxes from Scots pine by surface conductance and abiotic factors. PLoS ONE. 8: e69027, DOI: 10.1371/journal.pone.0069027.

Zhang, Y.J., Meinzer, F.C., Hao, G.Y., Scholz, F.G., Bucci, S.J., Takahashi, F.S.C., Villalobos-Vega, R., Giraldo, J.P., Cao, K.F., Hoffmann, W.A. and Goldstein, G., 2009. Size-dependent mortality in a Neotropical savanna tree: the role of height-related adjustments in hydraulic architecture and carbon allocation. Plant Cell Environ. 32: 1456–1466, DOI: 10.1111/j.1365-3040.2009.02012.x.

Zhao, M.S. and Running, S.W., 2010. Drought-induced reduction in global terrestrial net primary production from 2000 through 2009. Science. 329: 940–943, DOI: 10.1126/science.1192666.

Zolfaghar, S., Villalobos-Vega, R., Cleverly, J., Zeppel, M., Rumman, R. and Eamus, D., 2014. The influence of depth-to-groundwater on structure and productivity of *Eucalyptus* woodlands. Aust. J. Bot. 62: 428-437, DOI: 10.1071/BT14139.

8. Legends

Table 1. Summary of rainfall and net ecosystem productivity (NEP) for four years of study at the Mulga woodland. Data for 2010–2012 from Eamus *et al*. (2013) and Cleverly *et al.* (2013a).

Figure 1. Daily (a, b) and cumulative (c) precipitation in the Mulga woodland (a, solid line c) and the *Corymbia* savanna (b, broken line c).

Figure 2. Daily (a) and cumulative (b) evapotranspiration (ET) in the Mulga woodland (solid line) and the *Corymbia* savanna (broken line).

Figure 3. Daily (a) and cumulative (b) net ecosystem productivity (NEP) in the Mulga woodland (solid line) and the *Corymbia* savanna (broken line). Daily values are shown as the 3-day running average. Values of NEP that are larger than zero (dashed line) represent C uptake.

Figure 4. Daily cycle of NEP. Values represent hourly average ± standard error (s.e.) during January 2013.

Figure 5. Daily ecosystem water use efficiency (eWUE). Values were determined as NEP/ET and shown for days when ET > 0.2 mm d^{-1}. Values above zero (dashed line) represent photosynthetic eWUE, while increasingly negative values of eWUE represent increasing values of respiratory eWUE.

Figure 6. MODIS enhanced vegetation index (EVI) as a four-month running average.

Figure 7. Carbon stable isotope ratio ($\delta^{13}C$) of *Acacia* (squares) and *C. opaca* (circles) leaves in the Mulga woodland and across three habitats (Mulga patch, open savanna, transition) within the *Corymbia* savanna. Symbols show mean ± s.e.

862 Table 1. Summary of rainfall and net ecosystem productivity (NEP) for four years
863 of study at the Mulga woodland. Data for 2010–2012 are from Eamus et al. (2013) and
864 Cleverly et al. (2013a). Data for 2012–2014 are from this study.
865

Year	Rainfall ($mm\ y^{-1}$)	NEP ($g\ C\ m^{-2}\ y^{-1}$)
2010–2011	565	259
2011–2012	184	−4
2012–2013	193	−25
2013–2014	295	12

866
867

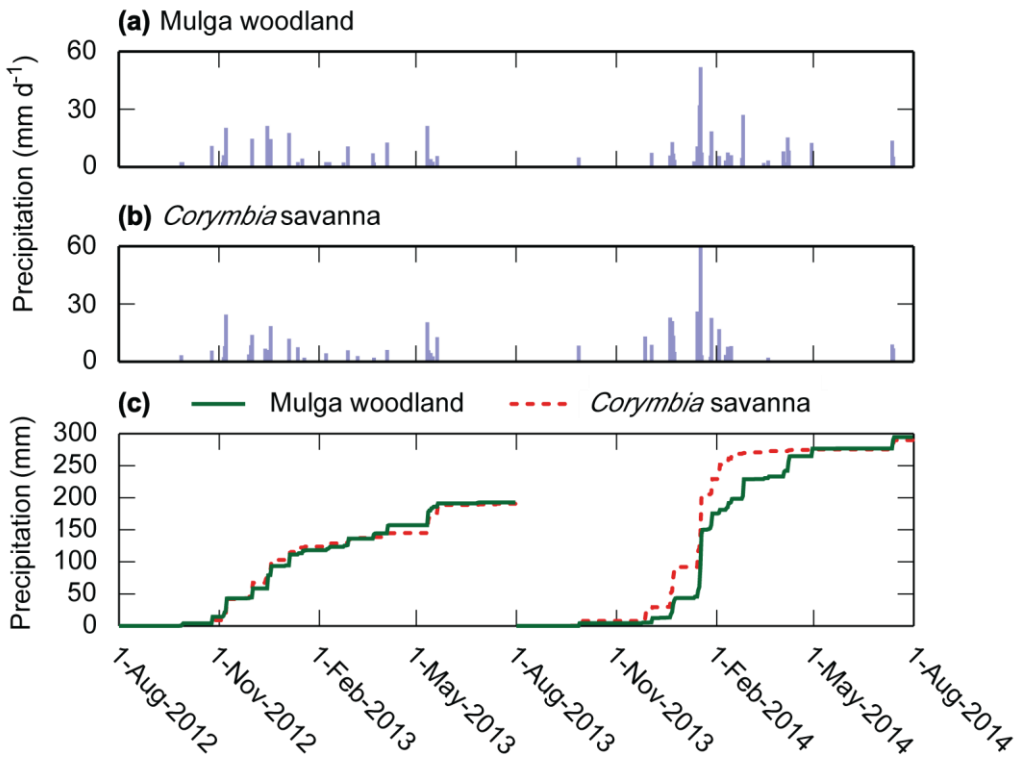

868

869 Figure 1. Daily (a, b) and cumulative (c) precipitation in the Mulga woodland (a,

870 solid line c) and the *Corymbia* savanna (b, broken line c).

871

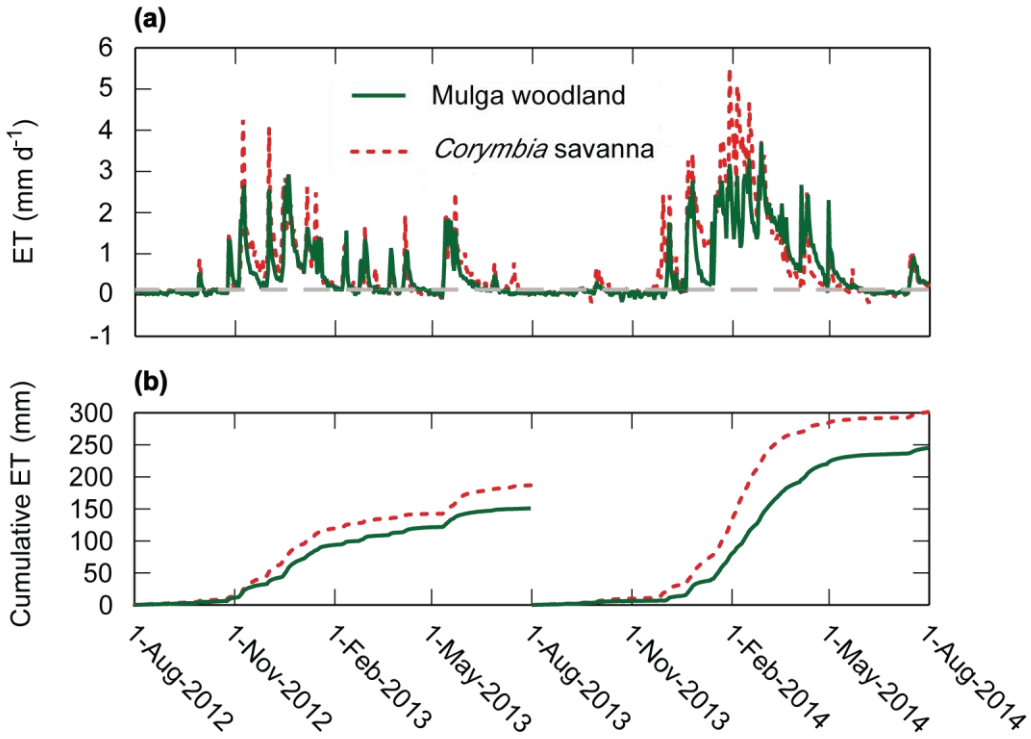

872

873 Figure 2. Daily (a) and cumulative (b) evapotranspiration (ET) in the Mulga

874 woodland (solid line) and the *Corymbia* savanna (broken line).

875

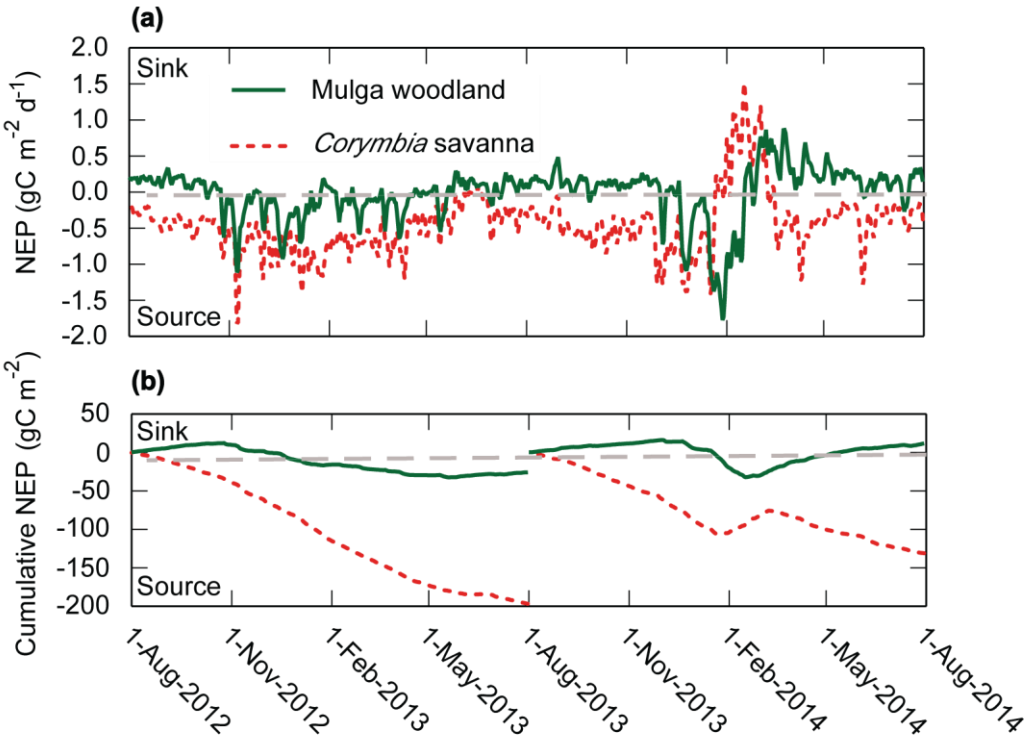

876

877 Figure 3. Daily (a) and cumulative (b) net ecosystem productivity (NEP) in the
878 Mulga woodland (solid line) and the *Corymbia* savanna (broken line). Daily values are
879 shown as the 3-day running average. Values of NEP that are larger than zero (dashed line)
880 represent C uptake.

881

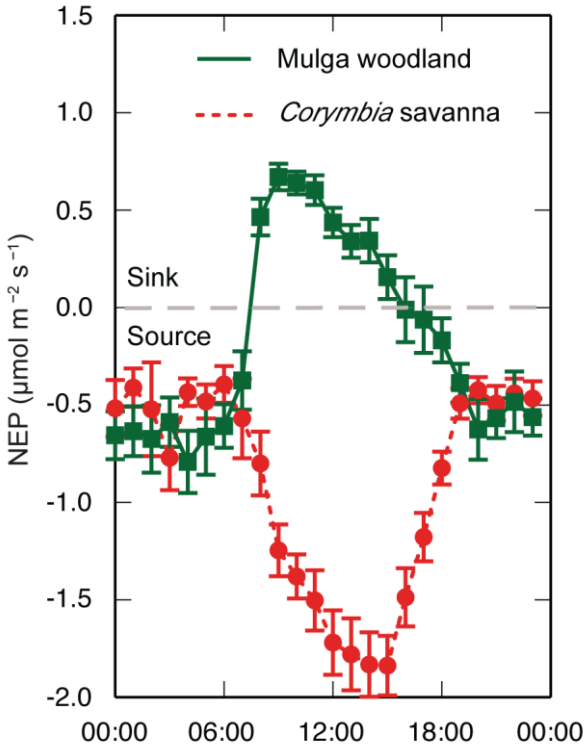

882

883 Figure 4. Daily cycle of NEP. Values represent hourly average ± standard error

884 (s.e.) during January 2013.

885

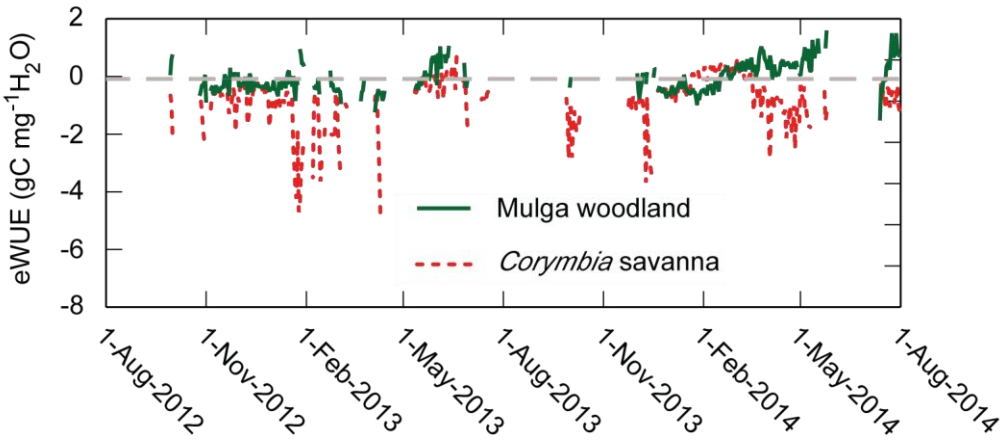

886

887 Figure 5. Daily ecosystem water use efficiency (eWUE). Values were determined

888 as NEP/ET and shown for days when ET > 0.2 mm d^{-1}. Values above zero (dashed line)

889 represent photosynthetic eWUE, while increasingly negative values of eWUE represent

890 increasing values of respiratory eWUE.

891

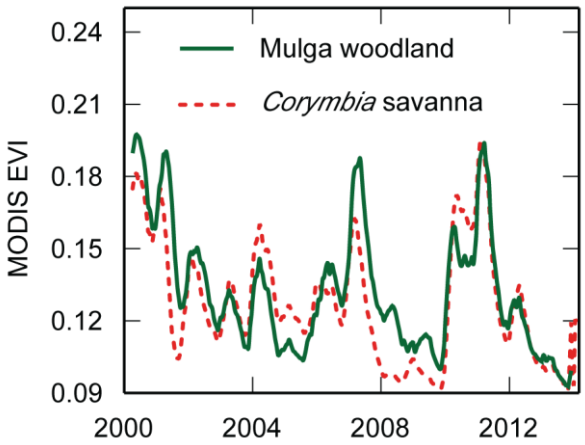

892

893 Figure 6. MODIS enhanced vegetation index (EVI) as a four-month running

894 average.

895

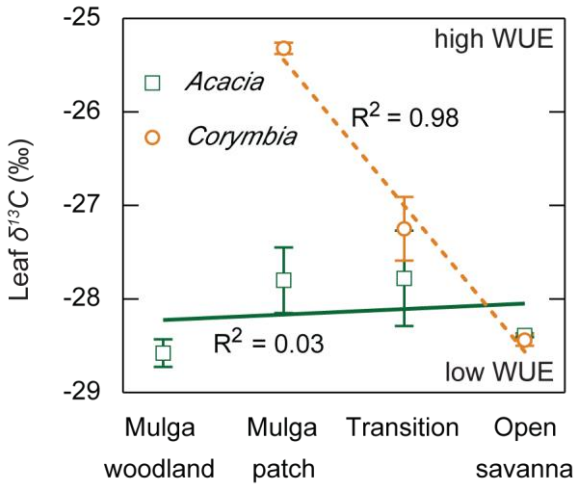

Figure 7. Carbon stable isotope ratio ($\delta^{13}C$) of *Acacia* (squares) and *C. opaca* (circles) leaves in the Mulga woodland and across three habitats (Mulga patch, open savanna, transition) within the *Corymbia* savanna. Symbols show mean ± s.e.